Image surface extremal points, new feature points for image registration

Jean-Philippe Thirion, Serge Benayoun

INRIA

INSTITUT NATIONAL DE RECHERCHE EN INFORMATIQUE ET EN AUTOMATIQUE

Image Surface Extremal Points, new feature points for Image Registration

Jean-Philippe THIRION, , Serge BENAYOUN

N° 2003

Août 1993

PROGRAMME 4

Robotique,
image
et vision

ISSN 0249-6399

Image Surface Extremal Points, new feature points for Image Registration

Jean-Philippe THIRION, *, Serge BENAYOUN **

Programme 4 — Robotique, image et vision
Projet Epidaure ***

Rapport de recherche n ° 2003 — Août 1993 — 32 pages

Abstract: We generalize the definition of the Extremal Points (EP) to image surfaces, and also to hyper-surfaces in any dimensions. These feature points can be used for image analysis and image registration because their relative positions are invariant with respect to rigid transforms. In a previous paper, we have defined the Extremal Points of the object surface for 3D Images, and we have shown how to extract those points, and how to use them to perform automatically the accurate registration of 3D medical images. The Extremal Points of the object surface are also invariant with changes of the image dynamic, because they are intrinsic to the object surface.

We show now that another kind of Extremal Points can be defined in 3D, from the 4D image surface $(x, y, z, f(x, y, z))$. We explain how to compute and extract those new Extremal Points, and then present registration experiments, comparing the results between the use of the Extremal Points of the object surface and of the image surface. We conclude by showing that both methods have their own advantages, leading to the extraction of extremely precise feature points and to the reliable registration of 3D images.

Key-words: 3D Image Processing, Registration, Differential Geometry, Geometric Invariant

*Email: jean-philippe.thirion@sophia.inria.fr
**serge.benayoun@sophia.inria.fr
***http://zenon.inria.fr:8003/Equipes/EPIDAURE-eng.html

Unité de recherche INRIA Sophia-Antipolis
2004 route des Lucioles, BP 93, 06902 SOPHIA-ANTIPOLIS Cedex (France)
Téléphone : (33) 93 65 77 77 – Télécopie : (33) 93 65 77 65

(Résumé : tsvp)

Les Points Extrémaux des Surfaces d'Images : nouveaux points caractéristiques pour le recalage d'images

Résumé : Nous généralisons la définition des Points Extrémaux aux surfaces d'images, et également aux hyper-surfaces en dimension quelconque. Ces points caractéristiques sont utilisables en analyse d'image et en recalage d'images, parce que leurs positions relatives sont invariantes par transformation géométrique rigide. Dans un article précédant, nous avions défini les Points Extrémaux de la surface objet, pour le cas des images 3D, et montré comment extraire et utiliser ces points pour le recalage automatique et précis des images médicales. Parce qu'ils sont intrinsèques à la surface de l'objet, ces points sont également insensibles à un changement d'intensité de l'image.

Nous montrons maintenant que l'on peut définir une autre classe de Points Extrémaux en 3D, à partir de la surface image 4D $(x, y, z, f(x, y, z))$. Nous expliquons comment calculer et extraire ces nouveaux Points Extrémaux, et présentons des expériences de recalage, afin de comparer les performances des Points Extrémaux de la surface objet et de la surface image. Notre conclusion est que chaque méthode a ses propres avantages, et conduisent toutes deux à l'extraction de points caractéristiques d'une extrême précision et au recalage automatique et robuste des images 3D.

Mots-clé : traitement d'images 3D, recalage, géométrie différentielle, invariant géométrique.

1 Introduction

Performing automatically the registration of 3D images is an important challenge for 3D Image Processing. The accurate 3D registration is the only way to fairly compare two scanner images of the same patient for diagnosis, and to estimate the evolution of a pathology. Another major challenge is the registration between two different patients, to compare the morpholological or physiological differences. At last, the registration of a patient with an anatomical atlas, which could be the average representation of an ideal patient, is the first step toward the automatic labeling of 3D images, and therefore their use in automated protocols.

We focus our studies on *intrinsic* registration methods, that is, methods which do not rely on external markers, but only on the image information. Petra van den Elsen, in [22], explains that intrinsic registration methods are likely to be more precise than methods using markers. Unfortunately, this assumption is hard to verify experimentally because we don't know what to consider as the ground truth for the real transform. Our own experience tends to confirm this.

In previous works, we have shown how to automatically extract the crest lines (or ridge lines) from 3D images with an original algorithm called the "Marching Lines" algorithm (see [19], [20]). Those crest lines are invariant with respect to rigid transforms, and can be used for the automatic registration (see [21], [5]). We have then introduced a new kind of feature points, the *Extremal Points*, in [18], which are particular points along the crest lines. Those points are defined from the differential characteristics of iso-intensity surfaces, and their relative positions are invariant with respect to a rigid transform. Because of this invariance, the Extremal Points can be used to perform the registration of 3D images of the same patient with a sub-voxel precision, and, because some of those points appear also to be anatomical landmarks, they seem very promising for measurement and registration between different patients. The reliability of those Crest Lines and Extremal Points is illustrated by the figures 6 and 7.

In those previous works, we focused on the properties of the surface of the object, which implies some kind of segmentation, which can be as simple as iso-intensity extraction (a simple threshold of the image), or more evolved methods making use of mathematical morphological operators, filtering, or the search of connected parts.

In the present paper, we investigate the differential properties of the 4D hyper-surface corresponding to the image intensity function, and we show how to define and extract Extremal Points from this hyper-surface. Then we show that those new feature points too can be used to perform the accurate registration of the 3D images. This leads us to extend the definition of Extremal Points to space of any dimension d, and to distinguish between the Extremal points of the object surface and of the image surface.

We show then experiments on real clinical data, to compare the performances of the registration with the different kinds of 3D Extremal Points.

2 The registration of 3D images

2.1 Different types of images to register

We must distinguish between several cases of registration, depending on the kinds of images to register.

- Mono-modal (versus multi-modal) qualifies operations performed with images issued from the same acquisition device, with the same parameter settings.
- Mono-subject (versus multi-subject) qualifies operations performed with images of the same physical object or patient.

In any case, the extraction of very precise and reliable landmarks is of an extreme importance. If we are looking for methods which are relatively independent from the subject scanned, they can't be based on anatomical landmarks, which are subject Dependant, but on geometric invariants. Fortunately, it appears that a significant subset of the geometrical landmarks that we automatically extract with our methods are also anatomical landmarks, as defined by the physicians, such as foramens, orbits, sub-mandibular lines...

At last, we are also to distinguish between morphological modalities, such as Magnetic Resonance (MR) scans and X-ray scans (cat-scan), and physiological modalities, such as Single Photon Emission Tomography (SPECT) or Positron Emission Tomography (PET) : the methods presented here are relevant for high resolution isotropic images, such as MR or X-ray, but not for low resolution physiological modalities such as SPECT or PET.

2.2 Existing image registration methods

The majority of the previous works, dealing with 3D image registration, are surface to surface matching methods (for example in [16], [2], [1], [9], [10], [6]). Among those methods, the best results seemed to be achieved with potential based methods (see [2], [9], [10]). In those methods, the surface of the scanned object is segmented from a reference image, and a force field is computed, based on the distance to the closest point of the surface. A second surface is extracted from the image to register, and the laws of the dynamic are applied to this surface, according to the force field. Those methods search the global minimum of this potential function, which occurs when the reference surface and the surface to register exactly fit. This kind of approaches give good results, even for multi-modal registration (for example NMR and PET, in [9]). However, those methods are generally only semi-automatic (subject dependent), because of the step of the segmentation of the surface.

There are very few results making use of other features than surfaces for registration, such as characteristic lines or points, other than methods using manually labeled images, or external markers. This is due to the difficulty to characterize feature lines and points in an automatic and reproducible way in 3D images. In [18], we emphasize the advantages of using 3D characteristic lines over surfaces, and of using 3D feature points over feature lines, when those features can be extracted reliably. Mainly, the advantages are the compactness of the representation, and that a matching based on a line to line distance or on a point to point distance is *much well defined* than for a surface to surface distance method.

Most of the registration methods designed for surface to surface matching, including potential based methods, can be adapted to the case of points or lines features. New ones, such as those presented in [5] or in [18], can be dedicated to lines, or points, and can make use of more complex processes, because those models are much more compact than the surface representation.

We think however that the geometric boundaries of objects for physiological modalities, such as SPECT or PET, are generally too much instable for using crest lines or extremal points methods, which restrict those methods to high quality images such as CAT-scan or NMR images. For those two last kinds of images, the method presented in [18] allows the *fully automatic* registration in the mono-modal, mono-subject case, and for a broad class

of subjects. There is still more work to do for multi-modal or multi-subject registration with this technique.

3 Definition of the image surface Extremal Points

We first recall some other works making use of differential geometry for image registration and segmentation. We recall the definition of object surface Extremal Points, and explain how to define extremal points for hyper-surfaces in spaces of any dimension d. Then we define the Extremal points of the 3D image surfaces, and show how to automatically compute and extract them.

3.1 The Extremal Points for 3D surfaces

Differential geometry has been successfully used for 2D image processing, for the extraction of *corner points*, which are sometimes defined as the points with the highest curvature along iso-intensity contours (see [7]) or as singularity of the image surface $z = f(x, y)$ (see [15], [4]). Differential geometry can be used also to characterize the object boundary, as described in [22], and to characterize crest lines (see for example [13], [19]). The generalization of corner points to arbitrary dimension d can be either ridges hyper-lines (a varieties of dimension $d-2$), as defined in [14], or singular points (a variety of dimension 0), as defined in the present paper.

Let us recall briefly some of the differential geometry properties of 3D surfaces. At any point P of a (2 times differentiable) 3D surface, one can define an infinite number of curvatures, in fact one curvature $k_{\vec{t}}$ for each direction $\vec{t}$ in the tangent plane of that surface at P. There are two principal directions $\vec{t_1}$ and $\vec{t_2}$, whose associated curvatures k_1 and k_2, are called the principal curvatures. Those two curvatures are the extrema of all the curvatures which can be computed at point P (therefore the principal directions are not defined for the umbilic points, where the curvature is the same for any direction $\vec{t}$). By convention, k_1 is the maximal curvature in absolute value, and is simply called the *maximal curvature*. Along with the normal to the surface $\vec{n}$, $\vec{t_1}$ and $\vec{t_2}$ form an orthonormal basis.

Olivier Monga and al. have shown in [13] how to characterize crest lines points, being the local maxima of the maximal curvature of the surface.

They give an alternate definition, where those crest line points are the zero-crossings of a quantity called the *extremality function* e, which is the directional derivative of the maximal curvature, in the corresponding principal direction : in short $e = \vec{\nabla} k_1 \cdot \vec{t}_1$, where $\vec{\nabla}$ is the gradient operator, and "$\cdot$" the scalar product. We have presented in [19],[20] a way to automatically extract those crest lines with an new algorithm called the *Marching Lines* algorithm, which extracts the crest lines of iso-intensity surfaces from the 3D images : those lines are the intersection of two implicit surfaces, the first one being the iso-surface $f = I$, where f is the image function and I an iso-intensity constant, and the second one being the *crest surface* $e = 0$, where e is the extremality function.

At last, we have defined in [18] a new set of feature points on 3D surfaces, the Extremal Points, which are the points corresponding to the local extrema of both principal curvatures k_1 and k_2. We have characterized those points as being the zero-crossing of the following two extremality functions :

$$\begin{aligned} e_1 &= \vec{\nabla} k_1 \cdot \vec{t}_1 \\ e_2 &= \vec{\nabla} k_2 \cdot \vec{t}_2 \end{aligned} \tag{1}$$

To compute e_1 and e_2 for a 3D surface, one can use the classical formulae of the differential geometry of 3D surfaces, described for example in [3] or in [8]. These are well suited when the parametric representation of the surface $\vec{f}(u, v)$ is available, where u, v are the local coordinates, and $\vec{f}$ a 3D vector representing a point of the surface. This is the case when we consider a 2D depth map image $(x, y, f(x, y))$, or a 2D range data image. Then we can compute a 2D endomorphism, called the Weingarten endomorphism, whose eigenvectors are the principal directions, and whose eigenvalues are the associated principal curvatures.

In [20], we have shown how to compute those values (principal directions, curvatures and extremalities) when the surface is given in an implicit form $f(x, y, z) = I$, where I is a constant, and f the 3D image function. We use directly the differentials of f, up to order 3 (20 differentials), that we compute with the derivatives of Gaussian filters. We can then compute the Extremal Points of this iso-surface $f = I$, with sub-voxel precision, as the intersection of 3 implicit surfaces $f = I$, $e_1 = 0$ and $e_2 = 0$, as illustrated in figure 1.

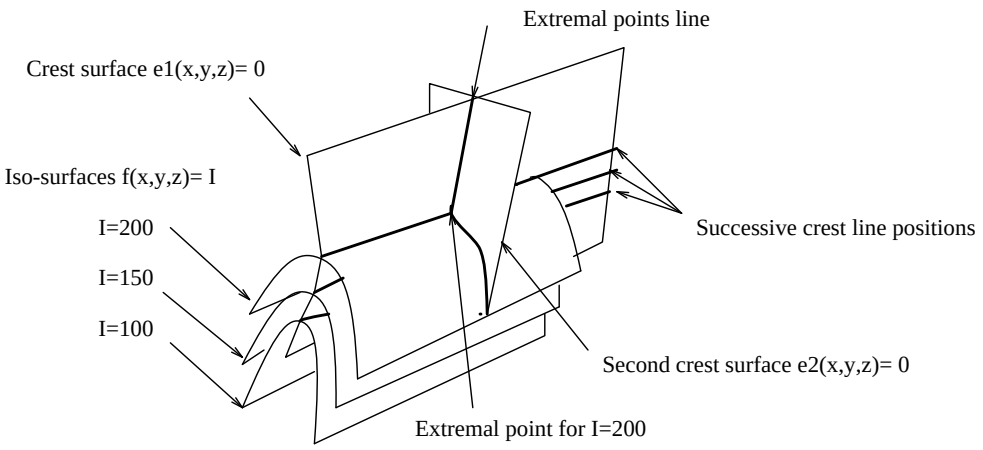

Figure 1: Definition of the object surface Extremal Points

3.2 Extension to any dimension

These results can be extend to a space of any dimension d. An hyper-surface in a d-space has $d-1$ principal directions $\{\vec{t_1}, \ldots, \vec{t_{d-1}}\}$, with $d-1$ corresponding principal curvatures $\{k_1, \ldots, k_{d-1}\}$, which can be ordered from the greatest to the smallest one in absolute value. The Extremal Points of this hyper-surface are the solutions of the $d-1$ implicit equations, corresponding to the simultaneous zero-crossings of the $d-1$ extremality functions $\{e_1, \ldots, e_{d-1}\}$, where $e_i = \vec{\nabla} k_i \cdot \vec{t_i}$.

Once again, those points can be computed with either the parametric representation of the hyper-surface, or with the implicit representation. Formulae are easier to establish for the parametric representation, as we will see now for the 4D case.

3.3 Object surface and Image surface Extremal Points

There is two ways to consider an image in dimension d. One can consider it as the (sampled) representation of a d-dimensional continuous function $f(x_1, \ldots, x_d)$, or as the (sampled) representation of a parametric hyper-surface in dimension $d+1$, $(x_1, \ldots, x_d, f(x_1, \ldots, x_d))$. For example, a 2D

image can be considered to be a 2D function $f(x, y)$, or a 3D depth map $z = f(x, y)$. The first representation is useful to determine the boundaries of the scanned objects, for example with an iso-intensity extraction technique. This representation is well suited to access to the characteristics of the object scanned : the same object, scanned with two different modalities, is likely to produce similar iso-contours.

On the contrary, the second representation (the image surface) depends strongly on the modality of the acquisition : two images of the same object with two different acquisition devices can produce very different image surfaces.

This duality corresponds to the duality implicit-explicit of surface representations. Invariants defined on iso-intensity boundaries are related mostly to the shape of the object, and can be computed with the implicit function theorem, whereas invariants defined on the image surface, which is a parametric representation, can be computed with the parametric formulae, but are very dependent on the acquisition modality : even the multiplication of the intensity with a constant value changes the geometric characteristics of the image surface.

3.4 The Extremal Points of 3D image surfaces

Let see now how to define and compute the 3D Extremal Points of the image surface of a 3D image, which is a 4D hyper-surface (the equations for object surface Extremal Points for 3D images can be found in [18]). O. Monga and S. Benayoun have shown in [12] how to define and compute the first and second fundamental forms F_1 and F_2 for 4D hyper-surfaces, from the differential of the 3D image, up to order 2. We recall those formulae here :

$$F_1 = \vec{\nabla} f \vec{\nabla} f^{\perp} + I = \begin{bmatrix} 1 + f_x^2 & f_x f_y & f_x f_z \\ f_x f_y & 1 + f_y^2 & f_y f_z \\ f_x f_z & f_y f_z & 1 + f_z^2 \end{bmatrix} \tag{2}$$

$$F_2 = -\frac{\mathcal{H}}{\sqrt{1 + \vec{\nabla} f^2}} = -\frac{1}{\sqrt{1 + f_x^2 + f_y^2 + f_z^2}} \begin{bmatrix} f_{xx} & f_{xy} & f_{xz} \\ f_{xy} & f_{yy} & f_{yz} \\ f_{xz} & f_{yz} & f_{zz} \end{bmatrix} \tag{3}$$

Where f is the image surface function, $\vec{\nabla} f = (f_x, f_y, f_z)$ is the image gradient, and $\mathcal{H}$ the Hessian of f. The expression W of the Weingarten endomorphism is then :

$$W = F_2 F_1^{-1} \tag{4}$$

These formulae can be also extended to any dimension d (see [17]). In our case, there are 3 principal directions $\vec{t_1}, \vec{t_2}, \vec{t_3}$ and 3 corresponding principal curvatures k_1, k_2, k_3, being respectively the eigenvectors and the eigenvalues of this endomorphism W. The computation of those values from the differentials of f, up to order 2, is detailed in the annex. We have established, after extensive calculation, the developed formulae which give the 3 extremality values e_1, e_2, e_3 from the differential of the 3D image, up to order 3 (we have programmed those functions, too lengthy to be written here) :

$$\begin{aligned} e_1 &= \vec{\nabla} k_1 \cdot \vec{t_1} \\ e_2 &= \vec{\nabla} k_2 \cdot \vec{t_2} \\ e_3 &= \vec{\nabla} k_3 \cdot \vec{t_3} \end{aligned} \tag{5}$$

The principal directions can be described with 4D vectors in the 4D space corresponding to the image hyper-surface, but the eigenvectors of the Weingarten endomorphism $\vec{t_1}, \vec{t_2}, \vec{t_3}$ are only 3D vectors. In fact, they correspond to the coordinates of the principal directions, given in the parametric space of the hyper-surface, which are simply the 3D conventional space coordinates (x, y, z). $\vec{\nabla}$ is also the gradient operator in the 3D conventional space.

3.5 Extraction of the image surface Extremal Points

The algorithm to extract those points is similar to the case of the objects surface : for the image surface, it is based on the intersection of three implicit surfaces $e_1 = 0$, $e_2 = 0$, and $e_3 = 0$, as illustrated in figure 2 (whereas it is $f = I$, $e_1 = 0$ and $e_2 = 0$ for the object surface case).

Therefore, these points can be extracted either with an extensive search through each voxels, or with the randomized implementation of the Marching Lines algorithm (see [20]), which can be used to reduce the complexity.

We just describe here the extensive computation algorithm : the following function is applied to each cell of the regular grid which constitutes the 3D image :

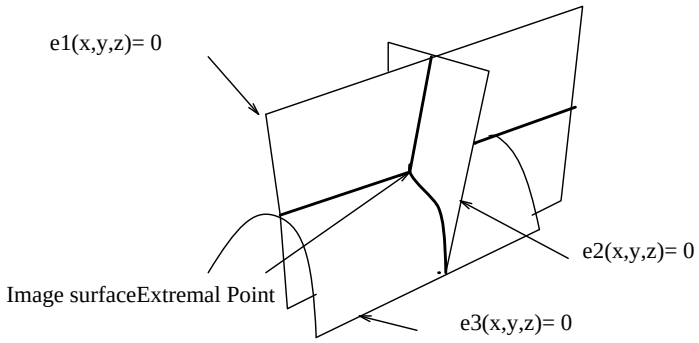

Figure 2: Definition of the image surface Extremal Points

- we compute for the eight vertices of this cell the values of the 20 differentials of the image f, up to order 3, with the convolutions of the image with the derivatives of the Gaussian function.
- we compute then the 3 extremality functions e_1, e_2, e_3 for those 8 vertices, with the extremality formulae of equations 5.
- If the signs of the 8 extremalities e_1 are the same, or if this is the case for e_2 or e_3, then we consider that there is no extremal point, and the processing of this cell is over.
- Else we compute, with linear interpolations, the position of the (possible) intersection points of the zero crossings of the 3 extremality functions (illustrated in figure 3, also detailed in [20]).
- At last, we can compute, with tri-linear interpolations in the cubic cell, the values of the 20 differentials of f for those intersection points, and re-compute such quantities as principal curvatures k_1, k_2, k_3 and principal directions $\vec{t_1}, \vec{t_2}, \vec{t_3}$ for those particular points.

The result is a set of 3D points, the Extremal Points of the image surface, with a set of associated attributes, the 3 principal curvatures and associated principal directions. Those attributes are invariant for the curvatures, and relatively invariant for the directions, with respect to rigid transforms, and

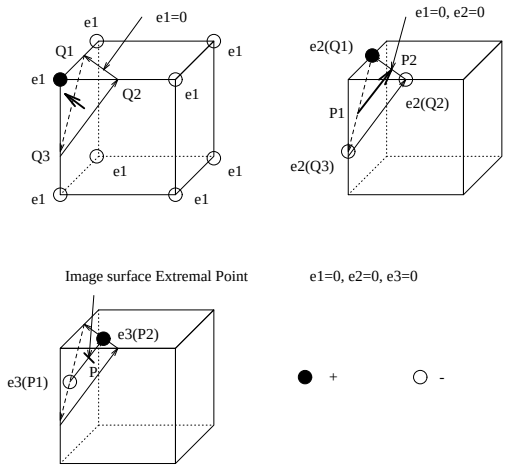

Figure 3: Example of image surface Extremal Points extraction

can be used efficiently to find corresponding points for image registration, in the same way than for the object surface Extremal Points.

Unfortunately, those points and their attributes are not invariant to a change of the dynamic of the images (even to a different scaling of the intensity), and therefore can't be used for multi-modal registration.

At last, these image surface Extremal Points are significant only in the vicinity of real contours. In uniform zones, such as the image background, many unstable extremal points may appear, due only to the noise. These can be eliminated with a test on the gradient norm, which can be used also to speed up the computation : extremalities are computed only when the gradient norm is significant.

4 Experimental comparisons

4.1 The registration method used in our experiments.

The present paper concentrates on feature points extraction, therefore we just describe briefly the registration method that we use in our experiments

: many other registration methods can be used, including potential based methods.

Our results however (the maximum number of points matched at a given distance), is an objective quantity which doesn't depend on the registration method, because the global minimum can't be mistaken with a local minimum when the probability that two points fall in the same bucket is less than $1/100th$ and thousands of points are matched (this is the strength of a point to point registration method). We use a simple prediction-verification scheme, which can be summarized as follow :

- We classify the Extremal Points into buckets, according to their invariant attributes, to associate points with similar attributes.
- We constitute then couples of associated pairs of points between the two models, taking into account new invariants (for example the distance between the points of a pair, or the relative orientation of the principal directions...)
- We constitute from those couples of associated pairs, associated triangles (one triangle from each model), each couple of associated triangles defines a unique 3D transform.
- We compute the rigid transform with a least square method based on the quaternions (see [1]). We verify and improve each transform found by the iterative application of this least square method : at each step, more points are matched, and used to compute the new transform. The process is halted as soon as the number of points matched doesn't increase.

The result is a rigid transform, and a list of corresponding points which participate to the computation of this final transform. Although this algorithm is very simple, it is very robust and fast (because of the high quality of the extracted feature points). It takes only a couple of seconds to compute the rigid transform.

4.2 Different kinds of Extremal Points.

We have implemented 4 different ways to extract Extremal points :

- *Iso-EPs* : are the object surface Extremal Points of a given iso-intensity surface : $f = I, e_1(f) = 0, e_2(f) = 0$. Each extraction is characterized by the iso-value constant I.

- *Lap-EPs* : the image is first transformed into a Laplacian image $\Delta f = f_{xx} + f_{yy} + f_{zz}$, and then the Extremal Points are computed with the iso-value 0 : $\Delta = 0, e_1(\Delta) = 0, e_2(\Delta) = 0$ (see figure 10 and 11). To remove the zero-crossings of the Laplacian due to the noise, we keep only the points where the gradient norm is sufficiently high.

- *LapIso-EPs* : the extremality coefficients e_1 and e_2 can be computed almost everywhere from the image function f, the intersection of the two corresponding crest surfaces are the Extremal Points lines (see figure 1). One can choose any other surface for the position of the object boundary. LapIso-EP make use of the zero-crossings surfaces of the Laplacian $\Delta f = 0$ as third surface : $\Delta = 0, e_1(f) = 0, e_2(f) = 0$ (whereas in Lap-EPs, Δf is used to compute *both* the extremalities and the iso-surface).

- *Hyper-EPs* : are the image surface Extremal Points of the 3D image, as described in the present paper : $e_1 = 0, e_2 = 0, e_3 = 0$. These are also thresholded using the gradient norm.

4.3 Experimental results

We have tried our different methods on two clinical 3D MR images, coming from the study of multiple sclerosis conducted at the Brigham and Women's Hospital, Boston, by Dr Kikinis (see [11]). This study rely on a data base of 800 3D MR images, for which extremely precise 3D registration is required. The original images are $256 \times 256 \times 54$ voxels, and we reduced them to $128 \times 128 \times 84$ (cubic) voxels for our experiments. There is one month between the two acquisitions *I1* and *I2*, and we have both the first and second echo images *echo1* and *echo2*. We have experimented the registration between the two "first echo" images *I1_echo1* and *I2_echo1*, to test mono-modal, mono-patient registration, and then the registration between *I1_echo1* and *I2_echo2* to test inter-modal registration.

The informations that we found to be relevant for those experiments are :

Extremal Points	Tot1	Tot2	Match	Var	Perc
Iso-EPs	368	385	144	0.413	38 %
Lap-EPs	3653	4176	1270	0.327	32 %
LapIso-EPs	1391	1420	301	0.349	21 %
Hyper-EPs	9762	10783	1378	0.405	13 %

Figure 4: Results with the different kinds of Extremal Points

- *Tot1 and Tot2* : the total number of extracted feature points in each image.
- *Match* : the total number of points matched at a distance lesser than 0.6 voxel.
- *Var* : the average of the distance between the points matched.
- *Perc* : the percentage of points matched.

The results are summarized in the figure 4, and proves the high quality of our registration methods. There is about 1.4 million voxels in each processed images, from which we extracted a few number of points (about 1 out of 3500 for the Iso-EPs method !), and from those points, about one third are registered at a distance less than 0.6 voxels. We give in annex the histogram of the distribution of the distances between matched points, along with the differences of principal curvature values, and principal direction angles, which give some hints about the reliability of those invariants quantities. For example, the precision on the principal directions is about 15 degrees. At last, we present the application of the transform found between the two 3D images, in figures 8 and 9.

As for the registration between *I1_echo1* and *I2_echo2*, we succeeded to registrate only the Laplacian Extremal Points, with only 80 points matched (i.e. about $1/100^{th}$). This shows that, although inter-modality registration is possible with this technique, more work is requested to use it reliably. We have started to study the behavior of the Extremal Points in the scale space to improve those results.

Quantitative comparison between the different kinds of Extremal Points is however not easy to draw : the Iso-EPs seem to have the best selectivity : fewer points, and a higher proportion of points matched, whereas Lap-EPs seem to have the best quality of matching (the lowest average of the distance between matched points), and Hyper-EPs give the highest number of points matched.

5 A qualitative comparison of the different Extremal Points

What are the respective advantages of the object surface and of the image surface Extremal Points ? when are we to use one or the other ?

We give here a classification of the extremal points that we described, according to several properties, which are : the CPU time requirement, the automaticity of the extraction, the precision for the registration, the usefulness for multi-modal registration, and the number of invariants produced.

- *CPU-time* : The Iso-EPs are the easiest to extract, and the randomized implementation of the Marching Lines algorithm is very fast. The bottle neck is a global pre-filtering of the image, which takes about 10mn for each 3D images, on a DEC-5000 workstation. The extraction of the Extremal points takes about 5 minutes each, and the registration part, only a few seconds. Note that the filtering can be performed efficiently with fine grain parallel hardwares, as for the computation of the Extremal Points, which is independent from voxel to voxel. The techniques based on the Laplacian images are more costly, because the Laplacian image must also be computed with linear filtering, along with the gradient norm image. Furthermore, there are more Lap-EPs to extract than Iso-EPs. The hyper-surface Extremal Points computation is the most costly, because the computation of the 20 differentials of the image is requested for each point where the gradient norm is sufficiently strong. It takes about 16 hours to extract those points for one image on a workstation (but it can be also very easily parallelized).

- *Automaticity* : Our methods of registration are fully automatic, except for the iso-intensity threshold for the Iso-EPs method, and the gradient

threshold for the other methods. The gradient norm threshold is easier to establish, by giving the proportion of points to consider (for example 30%). This threshold is not very sensitive, 20% or 40% will give very similar results.

- *Precision* : the precision is based on both the number of points matched, and on the average distance between the points matched. Although the computation of the final rigid transform, using a least square method, and based on all the points matched gives *extremely precise* results for any of those methods, the Hyper-EPs are noticeable by the number of matched points produced, and the Lap-EPs by both their number and their qualities (the best average distance).

- *Multi-Modality* : we have positive results only for the Lap-EPs, but we think that any kind of object based Extremal Points could be used for Multi-Modal registration. We are sure however that the Hyper-EPs can't be used for Multi-Modal registration, because even the scaling of the image intensity has some influence on the points localization.

- *Geometric Invariants* : there are 2 directions and 2 associated curvatures with each object surface Extremal Points, whereas there are 3 directions and 3 associated curvatures with the image surface EPs, which gives an advantage to the Hyper-EPs method. Those invariants may prove to be very discriminant and useful for inter-subject registration.

As we can see, each method has its own advantages (except perhaps LapIso-EPs, compared with Lap-EPs). We have summarized those qualitative properties in figure 5.

6 Conclusion

In this paper, we have extended the definition of the Extremal Points to any dimension spaces, and have shown that there is a qualitative difference between the Extremal Points of the object surface and of the image surface. We have shown also that, for the case of 3 dimensional images of the same subject, with the same modality, any kinds of Extremal Points can be

Extremal Points	CPU-time	Automatic	Precision	Multi-modal	Invariants
Iso-EPs	XX	X	X	?	2
Lap-EPs	X	XX	XXX	X	2
LapIso-EPs	X	XX	X	?	2
Hyper-EPs		XX	XX		3

Figure 5: Results with the different kinds of Extremal Points

used to perform automatically the registration with an *extremely high* precision. Furthermore, we think that the Extremal Points are very promising for inter-patient registration. We are currently studying the behavior of Extremal Points in the scale space, in order to reduce the number of Extremal Points which are extracted to those which are also stable through scale space. We hope that those points will be sufficiently stable from patient to patient to allow the automatic inter-patient registration.

Acknowledgment

We wish to thank Nicholas Ayache and Olivier Monga for stimulating discussions about the differential geometry of surfaces, Dr Ron Kikinis, from the Harvard Medical School for the 3D MR images of the brain. Part of this study has been supported by the Esprit Basic Research Action VIVA. Thanks also to Digital Equipment who provided us with fast computers.

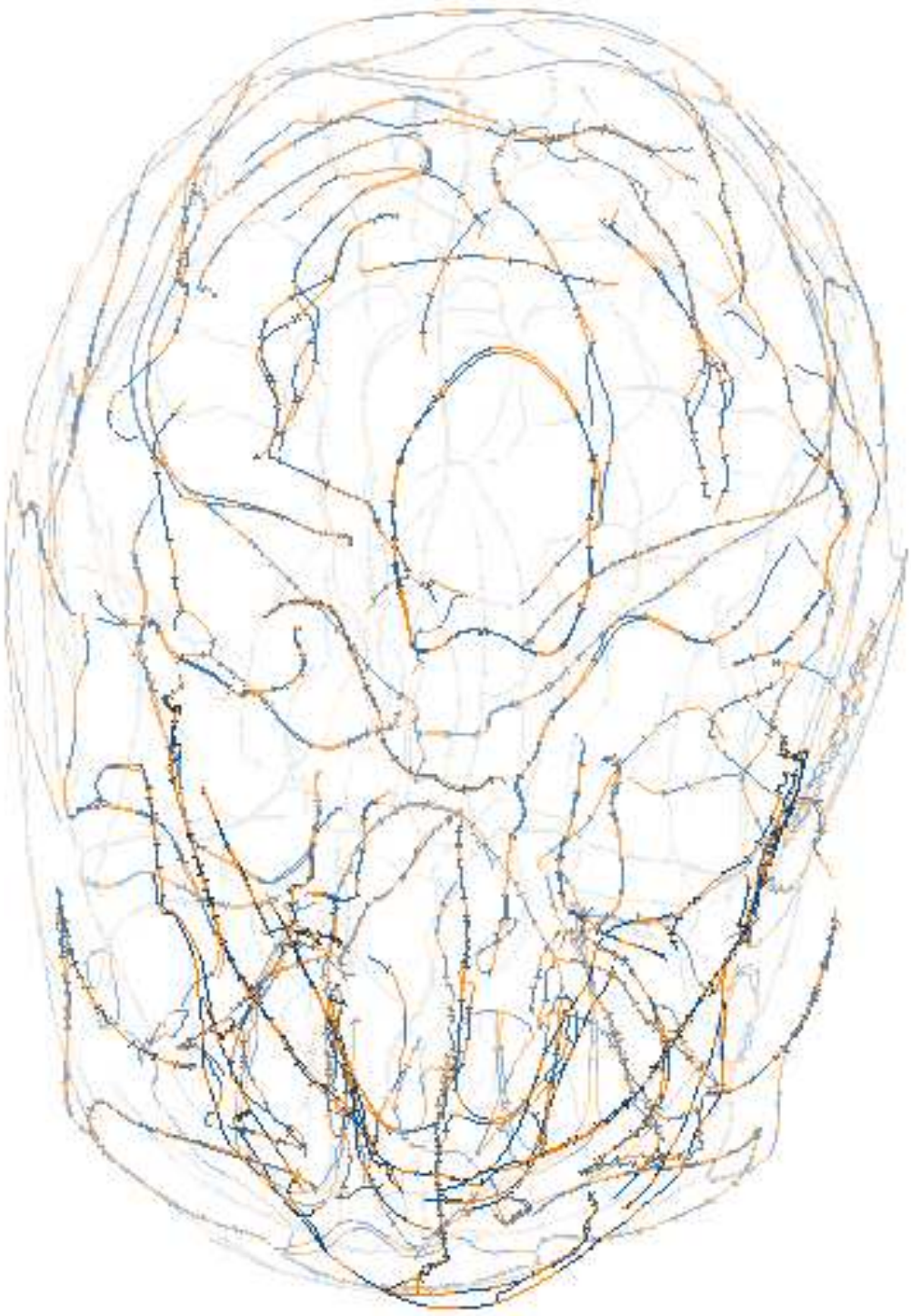

Figure 6: We have extracted and registered the Crest Lines and Extremal Points of two different scanner acquisitions of the same skull (160x200x140). In this figure, the Extremal Points are the loci of the crests where the color changes (Iso-EPs). The skull is viewed from bellow.

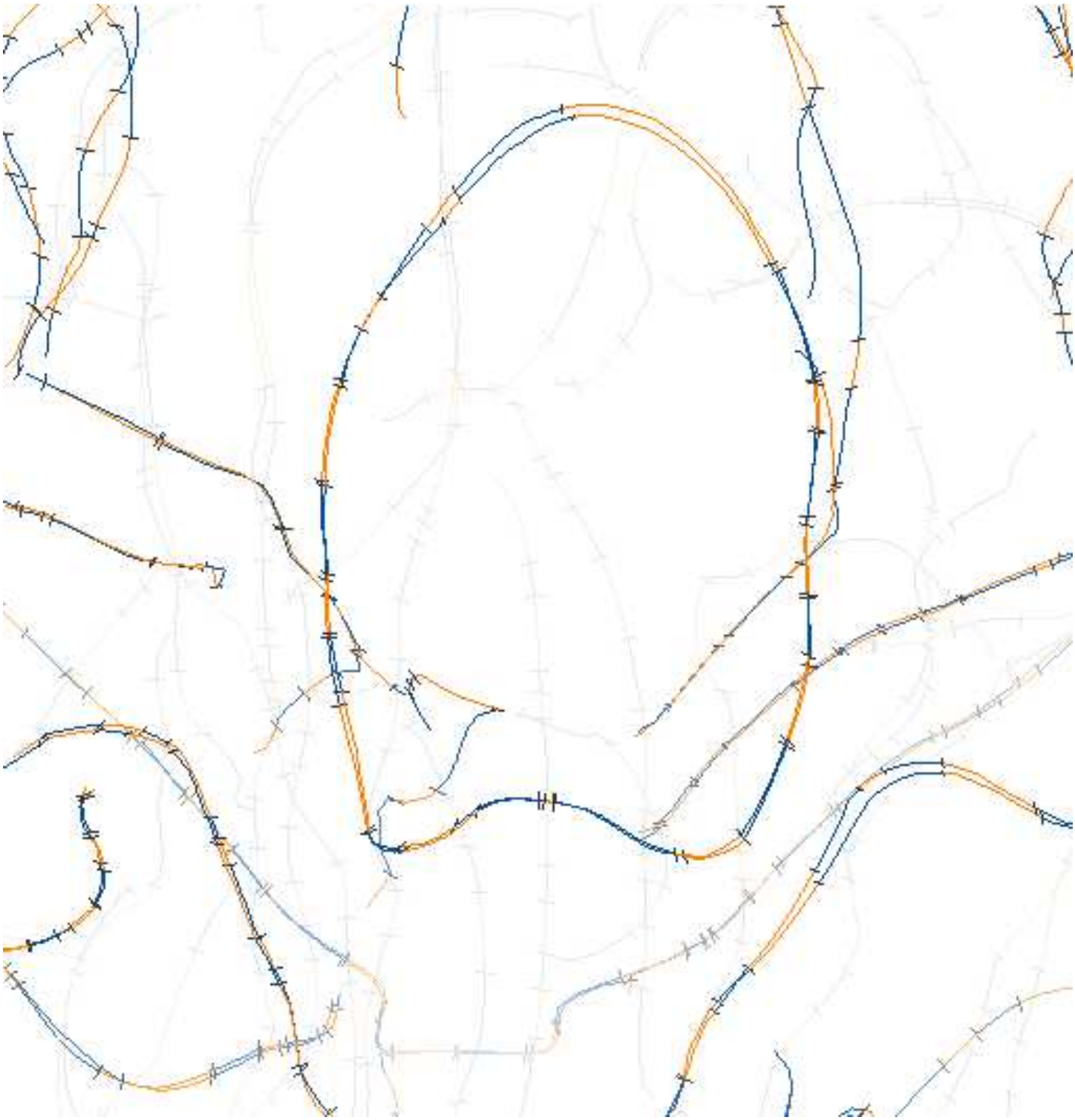

Figure 7: This figure represents a zoom at the level of the foramen occipital of the skull (connection between skull and spine), the two superimposed sets of crest lines are presented, corresponding to the two different acquisitions. This figure shows the tremendous accuracy of the Extremal Points positions : the width of the displayed lines is about 1/8th to 1/10th of the original voxel size.

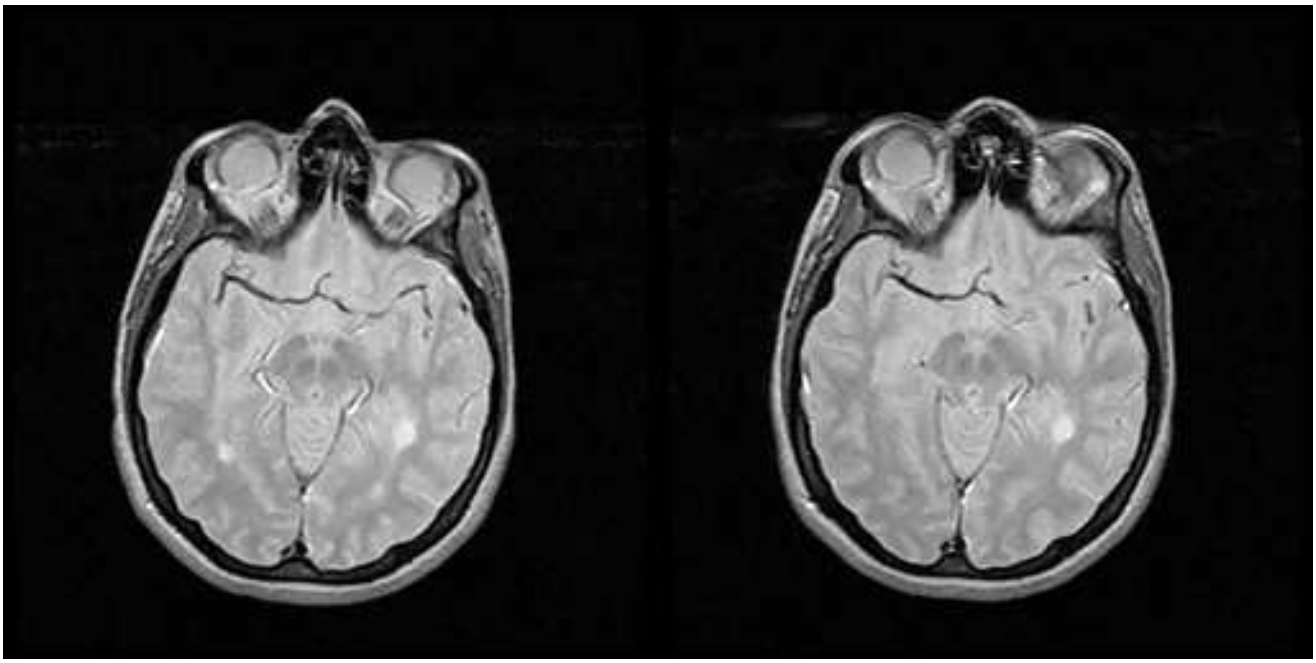

Figure 8: Two slices of the two 3D MR images before registration (the second slice is the closest from the first one). Differences are due to a slight difference of the vertical axis orientation. Multiple sclerosis appears as white spots in these images, a direct comparison may lead to diagnosis errors (for example, the blood vessel in the middle of the brain, in black, doesn't correspond between the two images).

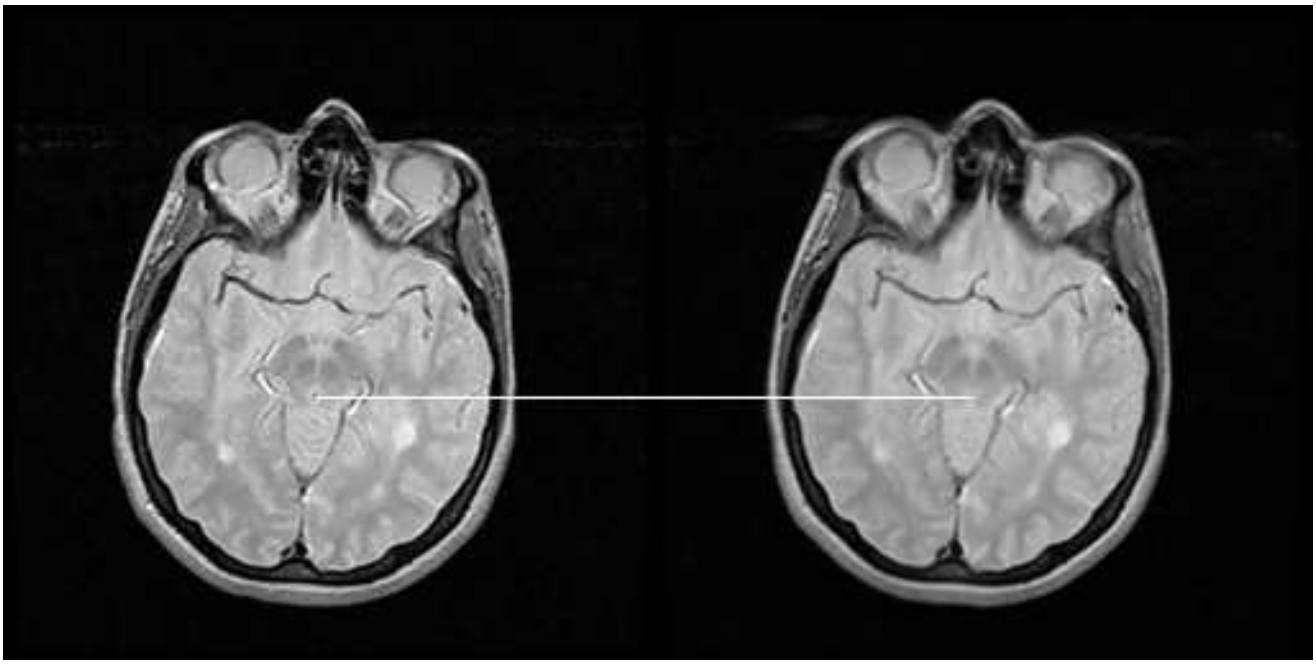

Figure 9: Two slices of the two 3D MR images after automatic registration, which can be used to evaluate the evolution of multiple sclerosis. The blood vessel (black, middle of the brain) has now a similar shape in both images.

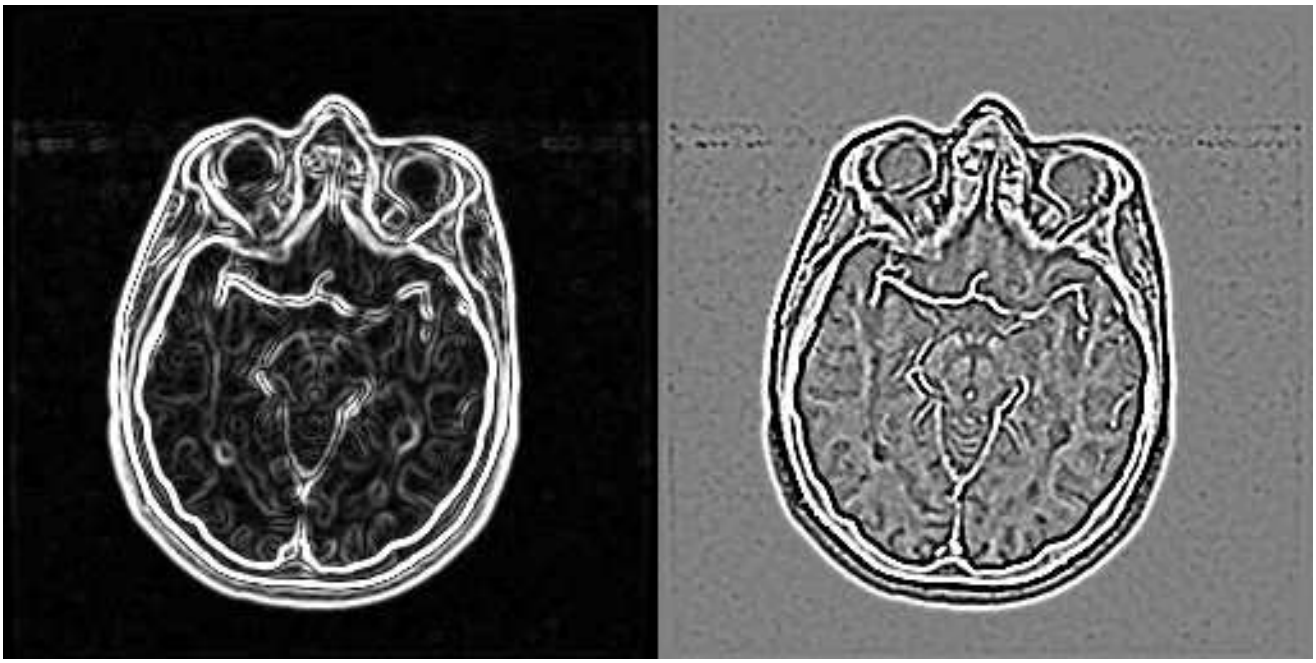

Figure 10: The gradient (left) and the Laplacian (right) of one slice. The zero-crossings of the Laplacian form surfaces in the 3D images whose localization can be more precise than simple iso-intensity surfaces. We have extracted the Extremal Points of those Laplacian surfaces (Lap-EPs method).

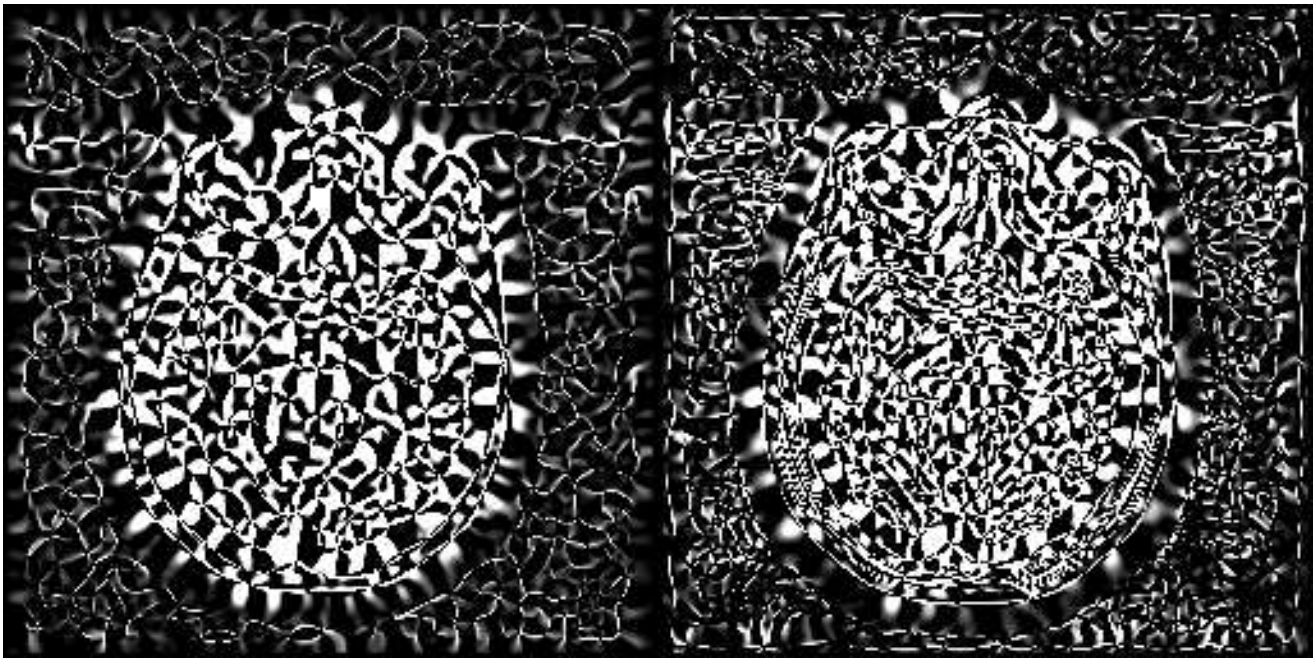

Figure 11: The image of the 2D extremality (left). The intersections between the zero-crossings in this image and the iso-contours in the original image give the *corner points*, which are the 2D equivalent of the Iso-EPs. Right is the 2D extremality of the Laplacian image. Those zero-crossings, along with the zero-crossings of the Laplacian, are the 2D equivalents of the Lap-EPs.

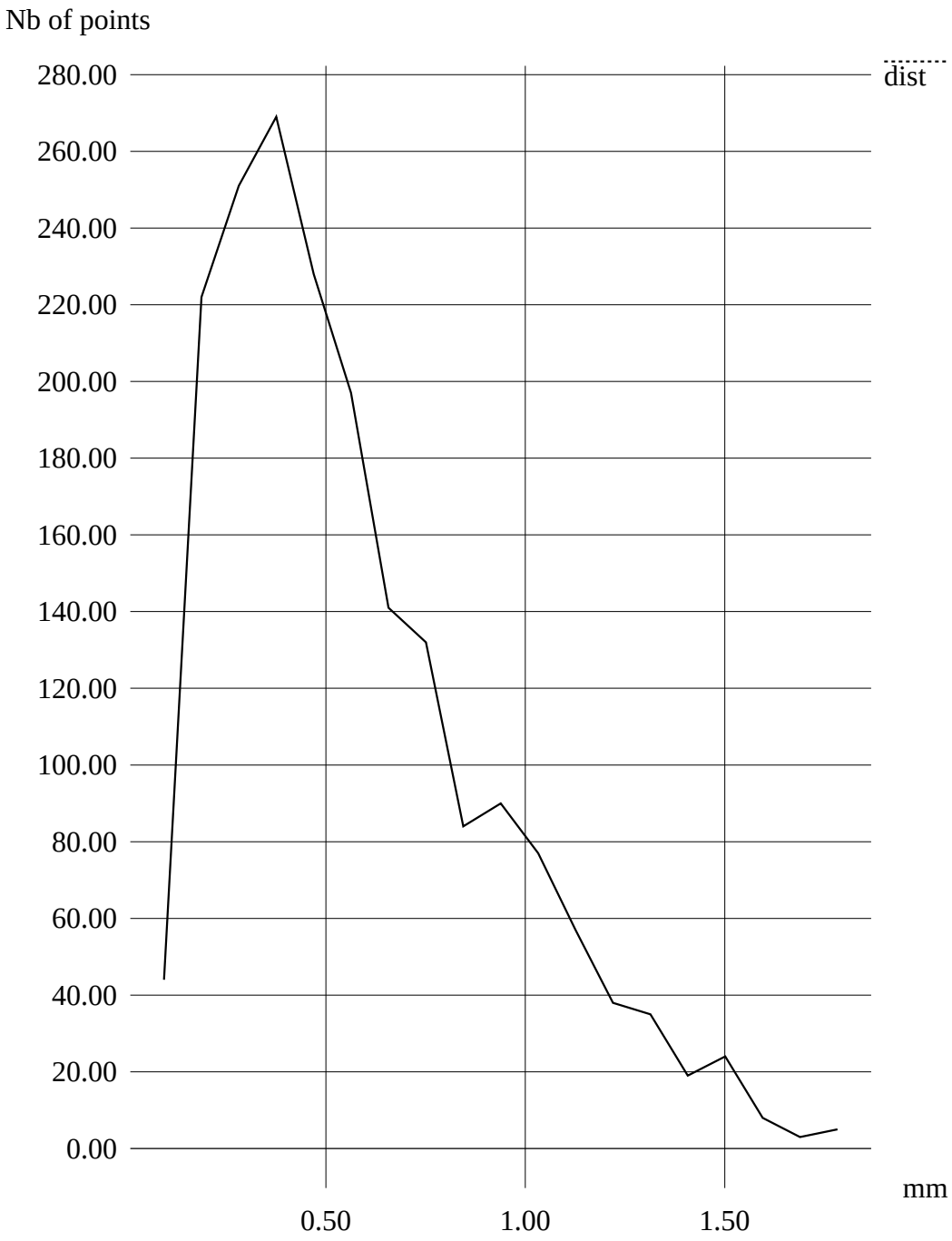

Figure 12: Distribution of the distances between matched points in millimeters (Lap-EPs)

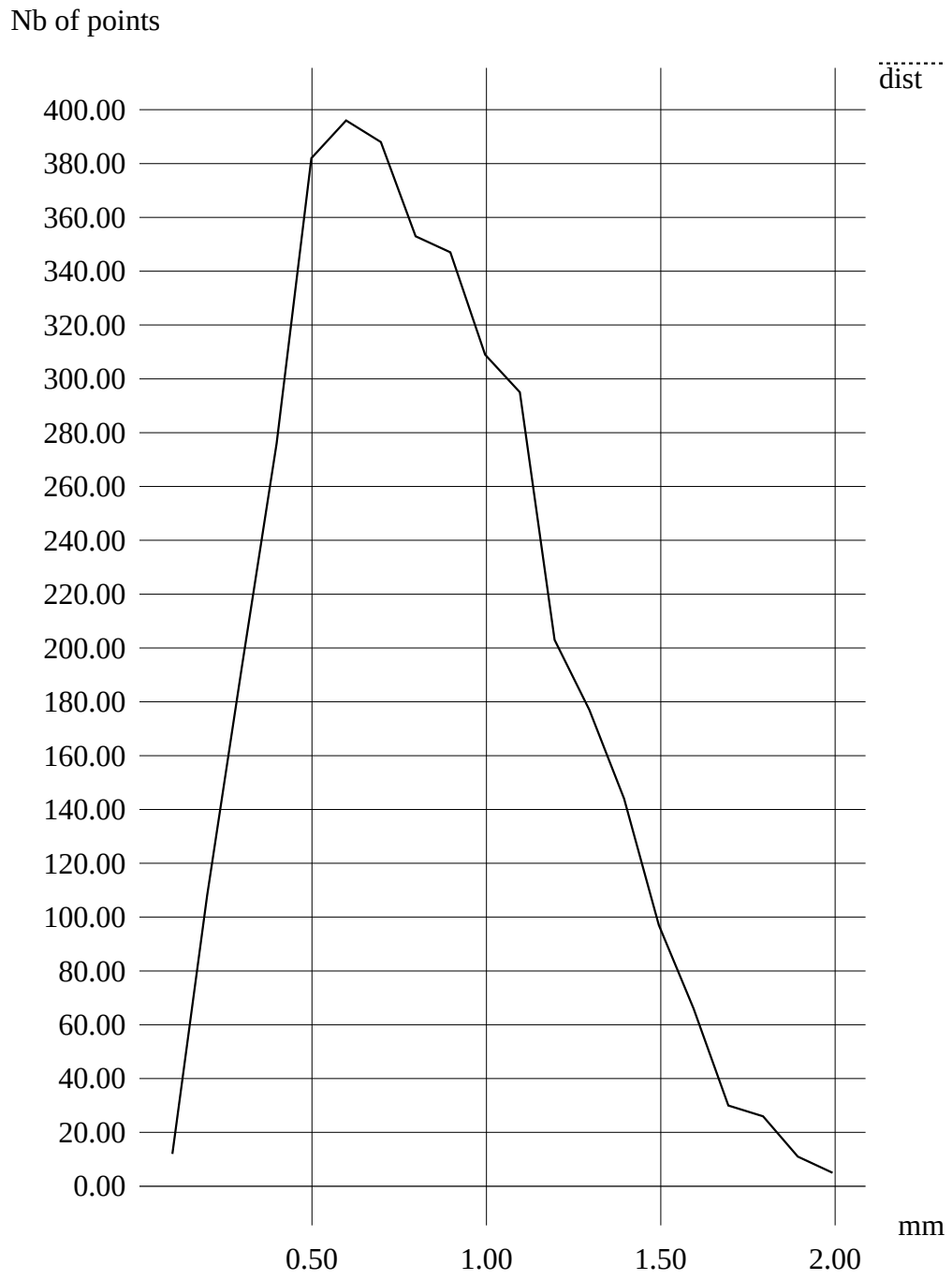

Figure 13: Distribution of the distances between matched points in millimeters (hyper-EPs)

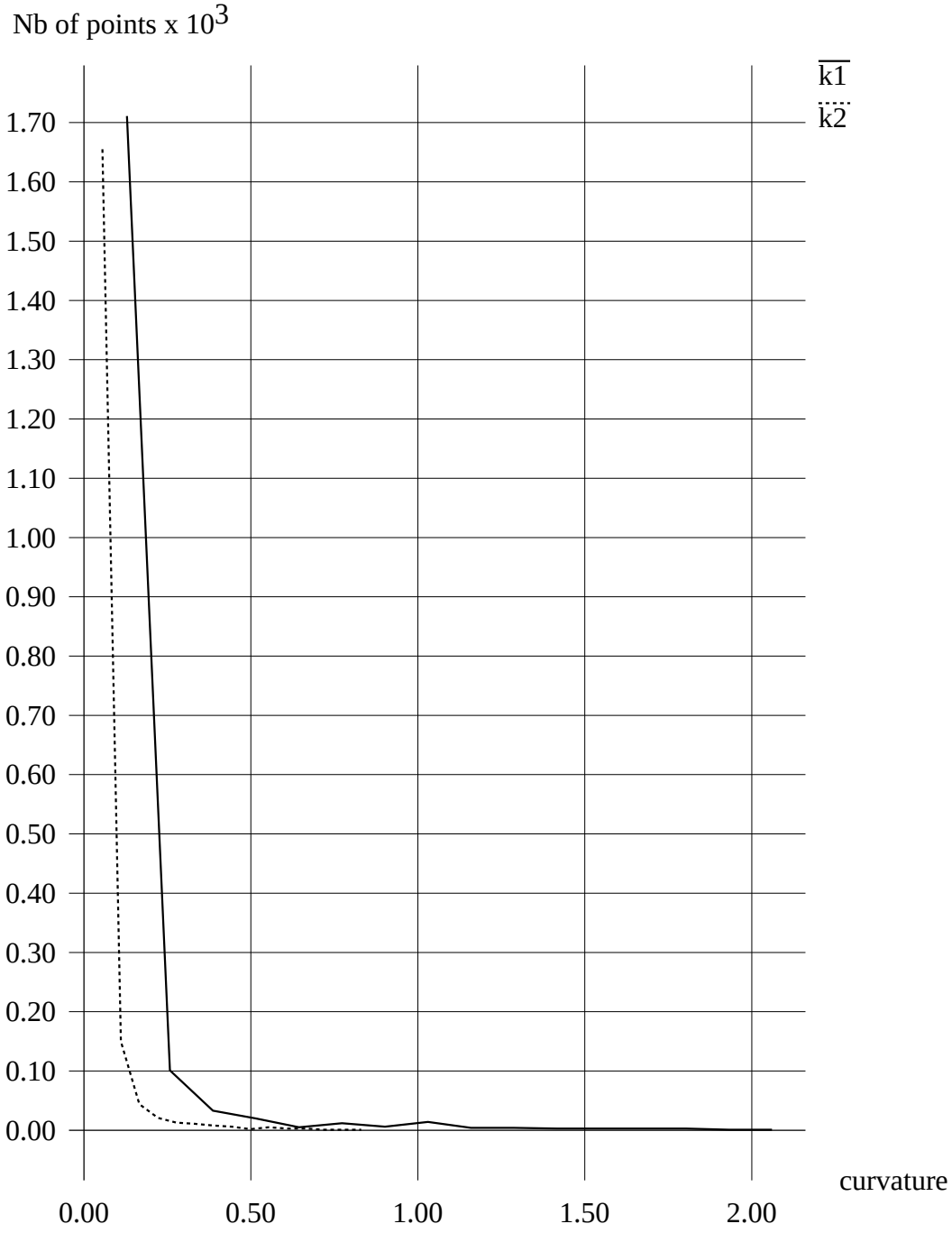

Figure 14: Distribution of principal curvature differences (Lap-EPs)

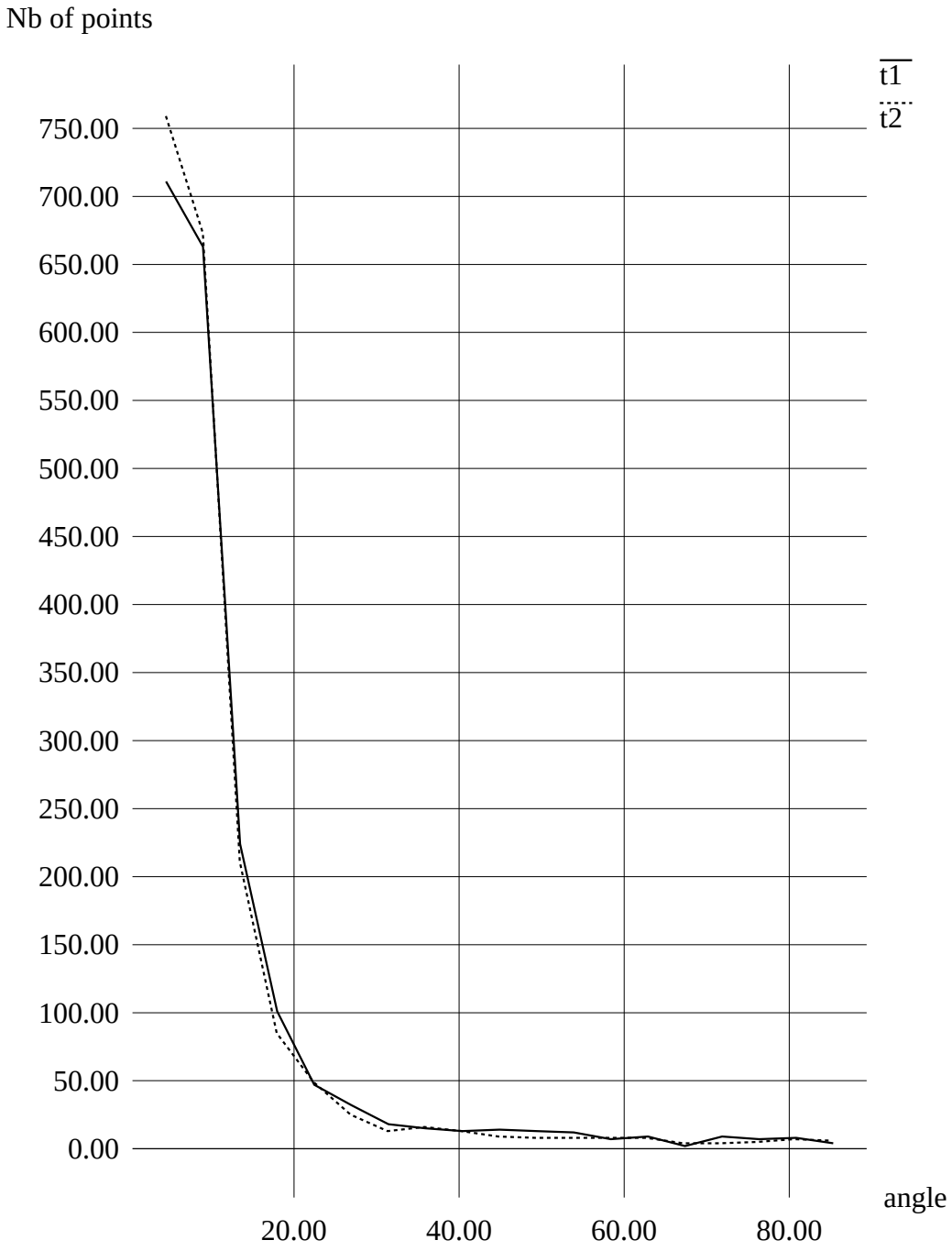

Figure 15: Distribution of principal direction differences in degrees (Lap-EPs)

Annex :

To compute explicitly the values of the principal directions and curvatures of the 4D image hyper-surface, we first compute the three following quantities K, H and M, where K is the determinant of the Weingarten endomorphism W, $3H$ is the trace of W, and M is the sum of the diagonal "minors" of W (2×2 sub-determinants of W). K is also called the Gaussian curvature, and H the mean curvature of the hyper-surface. We call *minor curvature* the value M.

The developed formulae of those three curvatures are :

$$K = \frac{f_{xx}f_{yy}f_{zz} + 2f_{xy}f_{xz}f_{yz} - f_{xx}f_{yz}^2 - f_{zz}f_{xy}^2 - f_{yy}f_{xz}^2}{(1 + f_x^2 + f_y^2 + f_z^2)^{\frac{5}{2}}}$$

$$3\,H = \frac{(1 + f_x^2 + f_z^2)f_{yy} + (1 + f_y^2 + f_z^2)f_{xx} + (1 + f_x^2 + f_y^2)f_{zz}}{(1 + f_x^2 + f_y^2 + f_z^2)^{\frac{3}{2}}}$$

$$- \frac{2f_xf_yf_{xy} + 2f_xf_zf_{xz} + 2f_yf_zf_{yz}}{(1 + f_x^2 + f_y^2 + f_z^2)^{\frac{3}{2}}}$$

$$M = \frac{(1 + f_x^2)(f_{yy}f_{zz} - f_{yz}^2) + (1 + f_z^2)(f_{xx}f_{yy} - f_{xy}^2) + (1 + f_y^2)(f_{xx}f_{zz} - f_{xz}^2)}{(1 + f_x^2 + f_y^2 + f_z^2)^2} +$$

$$\frac{2f_xf_y(f_{xz}f_{yz} - f_{xy}f_{zz}) + 2f_xf_z(f_{xy}f_{yz} - f_{xz}f_{yy}) + 2f_yf_z(f_{xy}f_{xz} - f_{yz}f_{xx})}{(1 + f_x^2 + f_y^2 + f_z^2)^2}$$

Replacing the image intensity f with $r \cdot f$, where r is an arbitrary constant is not without effect on the result, which shows that these results depends strongly on the dynamic of the image. We can observe that, if we consider points where the Laplacian $\Delta = f_{xx} + f_{yy} + f_{zz}$ of the image is zero (boundaries of the object), and if r tends toward ∞, then the mean curvature of the image surface tends toward the mean curvature of the object surface, and the minor curvature of the image surface tends toward the Gaussian curvature of the object surface (see [20] for the object surface formulae).

The principal curvatures k_1, k_2, k_3 are related to those three curvatures K, H, M in the following way :

$$\begin{array}{rcl} K & = & k_1\ k_2\ k_3 \\ 3\ H & = & k_1\ +\ k_2\ +\ k_3 \\ M & = & k_1k_2\ +\ k_1k_3\ +\ k_2k_3 \end{array} \tag{6}$$

Therefore, the principal curvatures are the solution of the following polynomial equation :

$$x^3 - 3Hx^2 + Mx - K = 0 \tag{7}$$

which becomes, with the following change of variables $y = x - H$:

$$y^3 + py + q = 0 \tag{8}$$

where

$$\left\{ \begin{array}{rcl} p & = & M\ -\ 3\ H^2 \\ q & = & M\ H\ -\ 2\ H^3\ -\ K \end{array} \right. \tag{9}$$

The discriminant is :

$$d\ = 27\ (\ 4\ p^3\ +\ 27\ q^2\ )\ = -27(k_1 - k_2)^2(k_1 - k_3)^2(k_2 - k_3)^2 \tag{10}$$

Which allows us to distinguish between 3 different cases:

$$(d = 0)\ et\ (p = 0) \Rightarrow (k_1 = k_2 = k_3 = H)\ \text{ umbilic point}$$

$$(d = 0)\ et\ (p \neq 0) \Rightarrow (k_1 = k_2 = \frac{-3q}{2p} + H)\ et\ (k_3 = \frac{3q}{p} + H)\ \text{ semi-umbilic}$$

$$(d < 0) \Rightarrow k_1, k_2, k_3 \text{ reel, distinct}$$

The 3 principal curvatures come from the roots of the complex number $z = \frac{-27q}{2} + i\frac{\sqrt{-d}}{2} = re^{i\phi}$, that is :

$$\begin{array}{rcl} k_1 & = & \frac{1}{3}\ (\alpha\ +\overline{\alpha})\ +\ H \\ k_2 & = & \frac{1}{3}\ (\overline{j}\alpha + j\overline{\alpha})\ +\ H \end{array}$$

$$k_3 \;=\; \frac{1}{3}\,(j\alpha + \overline{j}\overline{\alpha}) \;+\; H$$

with $j = e^{i\frac{2\pi}{3}}$ and $\alpha = \sqrt[3]{r}e^{i\frac{\phi}{3}}$.

The principal directions $\vec{t_1}, \vec{t_2}, \vec{t_3}$ can be computed by solving the linear system defined with the Weingarten endomorphism and the principal curvatures k_1, k_2, k_3.

The equations of the three extremality functions e_1, e_2, e_3 are obtained by differentiating the principal curvatures according to x, y and z. Therefore, e_1, e_2, e_3 can be explicitly computed from the differential of f, up to order 3 (we have programmed those formulae, which are too lengthy to be written here).

References

[1] P. J. Besl and N.D. McKay. A method for the registration of 3d shapes. *IEEE Trans. on Pattern Anal. and Machine Intell.*, 14(2):239–256, 1989.

[2] L. Brunie, S. Lavallée, and R. Szeliski. Using force field derived from 3d distance maps for infering the attitude of a 3d rigid object. *Proc. 2nd ECCV*, pages 670–675, 1992.

[3] Manfredo P. Do Carmo. *Differential Geometry of Curves and Surfaces.* Prentice Hall, 1976.

[4] Gerard Giraudon and Rachid Deriche. On corner and vertex detection. In *Conference on Computer Vision and Pattern Recognition*, Hawaii (USA), June 1991.

[5] A. Guéziec and N. Ayache. Smoothing and matching of 3D-space curves. In *Proceedings of the Second European Conference on Computer Vision 1992*, Santa Margherita Ligure, Italy, May 1992.

[6] H. Jiang, R.A. Robb, and K.S. Holton. A new approach to 3-d registration of multimodality medical images by surface matching. *Proc. SPIE Visualization in Biomedical Computing*, pages 192–213, 1992.

[7] Les Kitchen and Azriel Rosenfield. Gray-level corner detection. *Pattern Recognition Letters*, 1:95–102, 1982.

[8] Jan J. Koenderink. *Solid shape.* The MIT Press, 1990.

[9] G. Malandain and J.M. Rocchisani. Registration of 3d medical images using a mechanical based method. *Proc. 14th Int. Conf. IEEE EMBS, Sat. Symp. on 3D Advanced Image Processing in Medecine*, pages 91–95, 1992.

[10] J.F. Mangin, V. Frouin, and B. Bendriem. Nonsupervised 3d registration of pet and mri data using chamfer matching. *Medical Imaging Conf., Nuclear Science Symposium*, 1992.

[11] D. Metcalf, R. Kikinis, C. Guttmann, L. Vaina, and F. Jolesz. 4d connected component labelling applied to quantitative analysis of ms lesion temporal development. *IEEE EMBS*, November 1992.

[12] O. Monga and S. Benayoun. Using differential geometry in r^4 to extract typical surface features. *IEEE Conference on Computer Vision and Pattern Recognition*, June 1993.

[13] Olivier Monga, Serge Benayoun, and Olivier D. Faugeras. Using partial derivatives of 3d images to extract typical surface features. In *Proceedings CVPR '92, Urbana Champaign, Illinois.* IEEE, July 1992. also an INRIA Research Report (1599).

[14] B.S. Morse, S.M. Pizer, and Liu A. Multiscale medial analysis of medical images. *IPMI'93, 13th international Conference, Springer-Verlag*, Lecture Notes in Computer Science 687:112–131, 1993.

[15] Alison J. Noble. Finding corners. *Image and Vision Computing*, 6:121–128, 1988.

[16] C.A. Pelizzari, G.T.Y. Chen, Spelbring D.R., R.R. Weichselbaum, and C.T. Chen. Accurate three-dimensional registration of ct, pet, and/or mr images of the brain. *J. Comp. Assist. Tomog.*, 13(1):20–26, 1989.

[17] M. Spivak. A comprehensive introduction to differential geometry. *Berkley*, 1 to 5, 1971.

[18] J-P Thirion. New feature points based on geometric invariants for 3d image registration. *INRIA research report*, (1901 (submitted to IJCV)), April 1993.

[19] J-P. Thirion, N. Ayache, O. Monga, and Gourdon A. Dispositif de traitement d'informations d'images tri-dimensionnelles avec extraction de lignes remarquables. Brevet Français, numero 92 03900, Mars 1992. Pattent.

[20] J-P. Thirion and A. Gourdon. The 3d marching lines algorithm : new results and proofs. *rapport de recherche INRIA*, (1881 (submitted to CVGIP)), March 1993.

[21] J-P Thirion, O. Monga, Benayoun S., Gueziec A., and Ayache N. Automatic registration of 3d images using surface curvature. In *IEEE Int. Symp. on Optical Applied Science and Engineering*, San-Diego, July 1992.

[22] Petra Van den Elsen. Multimodality matching of brain images. *Utrecht University Thesis, the Netherland*, (ISBN 90-71546-02-0), 1993.

Unité de recherche INRIA Lorraine, Technôpole de Nancy-Brabois, Campus scientifique,
615 rue de Jardin Botanique, BP 101, 54600 VILLERS LÈS NANCY
Unité de recherche INRIA Rennes, IRISA, Campus universitaire de Beaulieu, 35042 RENNES Cedex
Unité de recherche INRIA Rhône-Alpes, 46 avenue Félix Viallet, 38031 GRENOBLE Cedex 1
Unité de recherche INRIA Rocquencourt, Domaine de Voluceau, Rocquencourt, BP 105, 78153 LE CHESNAY Cedex
Unité de recherche INRIA Sophia-Antipolis, 2004 route des Lucioles, BP 93, 06902 SOPHIA-ANTIPOLIS Cedex

Éditeur
INRIA, Domaine de Voluceau, Rocquencourt, BP 105, 78153 LE CHESNAY Cedex (France)
ISSN 0249-6399